TENTH AUSTRALASIAN FLUID MECHANICS
CONFERENCE - UNIVERSITY OF MELBOURNE
11-15 DECEMBER 1989

INTERACTIVE DYNAMICS OF STRAINED VORTICES

D.I. PULLIN and James D. BUNTINE*

Department of Mechanical Engineering
University of Queensland, St. Lucia, Qld. 4067
AUSTRALIA

ABSTRACT

Numerical simulations of the Navier-Stokes equations are used to study the interaction between M equal vortices embedded in an axisymmetric strain field which stretches vortex lines. Values M = 2, 3 and 4 are considered. As vortices merge and evolve towards an axisymmetric equilibrium state, complex patterns appear including the creation of strained shear layers and their subsequent destruction by viscous diffusion. The results of the simulations are used to calculate the form of the energy spectrum for a model of homogeneous turbulence consisting of an ensemble of merging strained vortices with M-fold interactions.

1. INTRODUCTION

The equilibrium vorticity distribution which results when a uni-directional vorticity field is subject to strain aligned with the vorticity, gives one of the more interesting fundamental solutions of the Navier-Stokes equations. In cylindrical (r,θ,z) co-ordinates with corresponding unit vectors $(\underline{r},\underline{\theta},\underline{k})$, let

$$\underline{\omega} = \omega(r,\theta,t)\underline{k} \ , \tag{1}$$

be the uni-directional vorticity field embedded in an imposed strain field with velocity

$$\underline{u}_s = -\tfrac{1}{2}\gamma r\underline{r} + \gamma z\underline{k} \ , \tag{2}$$

where γ is the constant strain rate. Then the axisymmetric equilibrium ω distribution is (Burgers 1948, Batchelor 1967)

$$\omega(r) = \frac{\Gamma\gamma}{4\pi\nu}\exp(-\frac{\gamma r^2}{4\nu}) \ , \tag{3}$$

where $\Gamma = 2\pi\int_0^\infty \omega r dr$ is the total circulation and ν is the fluid viscosity. Equation (3) gives a balance between viscous diffusion and strain-induced intensification of vorticity. Inertia plays no role.

Strained vortices like (3) have been used in turbulence modelling (eg Townsend 1951, Perry and Chong 1982, Lundgren 1982), and have been observed in numerical simulations of strained shear layers (Lin and Corcos 1984). Little is known however concerning either the fundamental dynamical interactions occurring between two or more strained vortices in close proximity, or the role such interactions might play in the mechanics of fine-scale turbulence. The aim of the present paper is to investigate these questions.

We study numerically the evolution of initial vorticity distributions consisting of a superposition of vorticity fields like (3), each offset from the centre of the strain field, and containing like-signed vorticity. The unsteady Navier-Stokes equations are solved numerically in stream-function vorticity formulation on an (r,θ)-plane using a hybrid spectral fourth-order finite-difference method. Configurations consisting of two, three or four vortices are considered.

2. FORMULATION

All flows considered have uni-directional vorticity like (1). The full velocity field is written as

$$\underline{u}(r,\theta,z,t) = \underline{v}(r,\theta,t) + \underline{u}_s \ , \tag{4}$$

where $\underline{u} = u_r\underline{r} + u_\theta\underline{\theta} + u_z\underline{k}$. In (4) $\underline{v}$ is the vortex induced velocity in the $(r-\theta)$-plane and $\underline{u}_s$ is given by (2). Since the fluid is incompressible, and $\nabla.(\underline{u}_s) = 0$, a stream function $\psi(r,\theta,t)$ associated with the $\underline{v}$ motion can be defined, where

$$\nabla^2\psi = -\omega \ , \tag{5a}$$

$$\underline{v} = \frac{1}{r}\frac{\partial\psi}{\partial\theta}\underline{r} - \frac{\partial\psi}{\partial r}\underline{\theta} \ , \tag{5b}$$

and $\underline{\omega} = \nabla\times\underline{v}$ .The vorticity transport equation, and the equation for ψ are respectively

$$\frac{\partial\omega}{\partial t} + u_r\frac{\partial\omega}{\partial r} + \frac{1}{r}u_\theta\frac{\partial\omega}{\partial\theta} = \gamma\omega + \frac{\nu}{r}\left\{\frac{\partial}{\partial r}\left(r\frac{\partial\omega}{\partial r}\right) + \frac{1}{r}\frac{\partial^2\omega}{\partial\theta^2}\right\}, \tag{6}$$

$$\frac{1}{r}\frac{\partial}{\partial r}\left(r\frac{\partial\psi}{\partial r}\right) + \frac{1}{r^2}\frac{\partial^2\psi}{\partial\theta^2} = -\omega \tag{7}$$

We wish to solve (5-7) numerically with given γ, and

$$\omega(r,\theta,t=0) \text{ given}, \tag{8a}$$

$$\omega(r\to\infty,\theta,t) \to 0, \ t \geq 0. \tag{8b}$$

Equation (3) together with an appropriate ψ may be shown to be an exact equilibrium solution to (5-7).

3. NUMERICAL SOLUTION

A combination of finite difference and spectral methods was used. We represent ω and ψ as

$$\omega(r,\theta,t) = \sum_{n=-\frac{N}{2}}^{\frac{N}{2}-1}\hat{\omega}_n(r,t)\,e^{in\theta} \tag{9a}$$

* Present address : Applied Mathematics, California Institute of Technology, Pasadena, CA 91125 USA.

$$\psi(r,\theta,t) = \sum_{n=-\frac{N}{2}}^{\frac{N}{2}-1} \hat{\psi}_n(r,t)\, e^{in\theta} \qquad (9b)$$

where $r \in [0,\infty)$, $\theta \in [0,2\pi)$ and N is a truncation parameter. Use of(9) in (5-7) gives evolution equations for $\hat{\omega}_n$ and $\hat{\psi}_n$, n= -N/2,...,N/2-1. Equation (7) gives N linear ODE's in r for the $\hat{\psi}_n$, given the $\hat{\omega}_n$. These were solved by a fourth-order finite difference method. Equation (6) gives N ODE's in t for the $\hat{\omega}_n$. These were integrated in t using a Crank-Nicolson two-point scheme which was fully implicit in the fourth-order spatially accurate linear terms. The $\nabla.(\omega u)$ terms were treated first by fourth-order differencing and direct multiplication on an NxN grid in the $(r-\theta)$-plane, and then by application of the discrete Fourier transform. Iteration on the nonlinear terms in each timestep Δt was required for stability. The boundary condition (8b) was implemented by the use of a tanh coordinate stretching transformation to map $r \in [0,\infty)$ onto a finite line. Very small time steps $\Delta t \cong 1/(N\,Re)$ were used. Solutions discussed presently have N =128. Further details of the numerical method including testing are given in Buntine and Pullin (1989).

4. RESULTS AND DISCUSSION

4.1 Vortex Merging

Physical quantities are made dimensionless by setting $\nu = 1$ and $\gamma = 4$ in numerical simulations. This sets to unity $\sqrt{4\nu/\gamma}$, the radius of the equilibrium vortex (3). A Reynolds number for the flow is defined as

$$Re = \Gamma/(2\pi\nu), \qquad (10)$$

where Γ is the total cirulation. We describe the results of three vortex merging simulations, each at Re = 640. In each calculation the initial conditions consist of a superposition, with M-fold asymmetry, of M = 1,2 or 3 vorticity fields, each like (3), but offset from the strain field centre by a distance d of order the individual vortex diameter. We suppose that these configurations model M-vortex interactions which might be typical events in a turbulence field where the imposed strain is provided by the average velocity field of surrounding compact vortices. Such alignment between a principal axis of the local strain field and vortex lines was found in numerical simulations of three-dimensional homogeneous turbulence by Ashurst *et al* (1987). The assumed asymmetry in the initial conditions is artificial but is adopted for simplicity.

The results of the simulations are displayed in figures 1-3 as timewise sequences of snapshots of the vorticity field. Since Γ is the same in each case, it may be expected that the asymptotic state of each simulation, when t becomes large will be the same equilibrium strained vortex solution given by (3).

In figure 1 the vortices first rotate about their mutual centre while each is deformed into a near elliptical shape by the local (r,θ)-plane strain field induced by its neighbour. Differential rotation produces spiral shear layers which roll-up. This is followed by the action of viscosity in smoothing the radial oscillations in the vorticity field to produce a nearly axisymmetric core, and finally, the strain field drives the vortex towards the asymptotic form (3). Simulations with initial core separation distance much larger than the vortex core diameter showed that the final phase of merging was influenced little by initial separation. The merging pattern of figure 2 may then be considered typical for a two-vortex merging event at moderate to high Re.

The three and four-vortex merging events of figures 2-3 show complex ω-distributions comprising multiple rotating shear layers. The last frames of figures 1, 2, and 3 clearly show unequal contour density for the three cases, at times when the merged vortex first becomes nearly axisymmetric. This indicates that for the M = 3 and M = 4 flows, the strain field requires more time to intensify the ω-field towards (3). This occurs on a time scale of order γ^{-1}, but takes longer with increasing M since, from (3), at t = 0, $|\omega_{max}| = \Gamma\gamma/(4\pi\nu M)$. By contrast th axisymmetrization time is order d^2/Γ for all M.

4.2 Turbulence Energy Spectrum

We consider a model of homogeneous turbulence comprising an ensemble of merging strained vortices. It may be imagined that the vorticity field consists of curved vortex rods with random orientation in three-dimensional space. In cross section each rod shows the structure of an M-fold strained vortex interaction at some time during its evolution. Such interactions may of course involve antiparallel vorticity leading to cancellation, but these events may be shown to make only a small contribution to an overall energy spectrum. Indeed the processes of merging and cancellation may be thought of as in balance at a particular Re, giving a stationary distribution. This model is essentially that considered by Townsend (1951), who used (3) as the fundamental solution, and Lundgren (1982) who considered a strained Kaden-spiral model. By replacing an ensemble average by a time average, it may be shown that for a quite general ω-distribution in the rod cross-section, the energy spectrum can be expressed as (Lundgren,1982, Buntine & Pullin 1989)

$$E(k) = \frac{\varepsilon}{2k\nu}\,\frac{P(k)}{M} \quad . \qquad (11)$$

$$P(k) = \int_0^{t_c} S(t)\left(I_0^2(k,t) + 2\sum_{n=1}^{\infty} |I_n^2(k,t)| \right) dt, \qquad (12)$$

$$I_n(k,t) = \int_0^{\infty} J_n(kr)\, \omega_n(r,t)\, r\, dr \quad . \qquad (13)$$

$$S(t) = \exp\left(\int_0^t \gamma(u)\, du \right) = e^{\gamma t} \quad , \qquad (14)$$

and

$$M = \int_0^{t_c} S(t) \int_0^{\infty} \left(\omega_0^{\,2} + 2\sum_{n=1}^{\infty} |\omega_n|^2 \right) r dr dt. \qquad (15)$$

In (11-15), k is the wavenumber, E the energy per unit mass per unit wavenumber, ε is the dissipation rate per unit mass and J_n is a Bessel function of the first kind of order n. Also t_c is a cutoff time for the merging which may be interpreted as the time required for axisymmetrization of the ω-distribution. We take $t_c = O(d^2/\Gamma)$.

To estimate ε, we identify γ with the root mean square strain rate. Dimensional arguments and the choice of an O(1) constant (Townsend 1951) then gives

$$4\gamma = \sqrt{\varepsilon/\nu} \quad , \qquad (16)$$

Putting $K = k/k_d$ where

$$k_d = 1/\eta = \left(\frac{\nu^3}{\varepsilon}\right)^{-1/4} \qquad (17)$$

is a wavenumber characteristic of the dissipation range and η is the Kolmogorov microscale, and using (16), the energy spectrum may be expressed in standard form (Hinze 1975) as

$$\frac{E(K)}{\left(\varepsilon\,\nu^5\right)^{1/4}} = \frac{8\,P(K)}{M\,K} \qquad (18)$$

In (18) P is given by (12), now nondimensionalized by the time and length scales given in section 2.

The energy spectrum in the form of (18) was obtained by calculating P(K) and M from (12-15), using the vorticity evolution data. The results are displayed in figures 4-6, for simulations with M = 2, 3 and 4 respectively. The two-vortex pairing result is compared with a similar calculation done at Re = 1280. The dissipation range (K > 1) shows good agreement with the Heisenberg K^{-7} law (see Hinze 1975) with M = 2 but less good agreement with M = 3 and M =4 : dissipation appears to be occurring in the rolled-up shear layers comprising the merged vortex core. There is no -5/3 range apparent although with M = 2 there is a flattened portion of the spectrum between the K^{-1} region at small K and the dissipation range.

5. CONCLUSION

The present model assumes that all merging events of the ensemble contributing to the spectrum evolve in an identical axisymetric strain environment, and at the same Re. The simulations of Ashurst *et al* however clearly indicate significant statistical variation in the principal components of the local rates of strain, and also in the orientation of the principal strain axes with respect to the local vorticity vector. In order to construct a convincing vortex-based model of inertial range turbulence, it may be neccessary to include information on the distribution of vortex and strain-rate scales taken up by the fluid, in a dynamically self consistent way.

This work was supported by the Australian Research Council under grant number A48315031.

REFERENCES

Ashurst, W.T., Kerstein, A.R., Kerr, R.M. and Gibson, C.H., 1987 *Phys. Fluids* **30** 2343

Batchelor, G.K.,1967 *An Introduction to Fluid Dynamics.* C.U.P.

Buntine, J.D. and Pullin, D.I., 1989 To appear in *J. Fluid Mech.*

Burgers, J.M.,1948 *Adv. Appl. Mech.* **1**, 171-199.

Hinze, J.O., 1975, *Turbulence,* 2nd edn. McGraw-Hill.

Lin, S.J. and Corcos, G.M., 1984 *J. Fluid Mech.* **141**, 139-178.

Lundgren, T.S., 1982, *Phys. Fluids,* **25**, 2193

Perry, A.E. and Chong, M.S., 1982 *J. Fluid Mech.* **119**, 123

Townsend, A.A., 1951. *Proc. R. Soc. Lond.* **A 208**, 534-540.

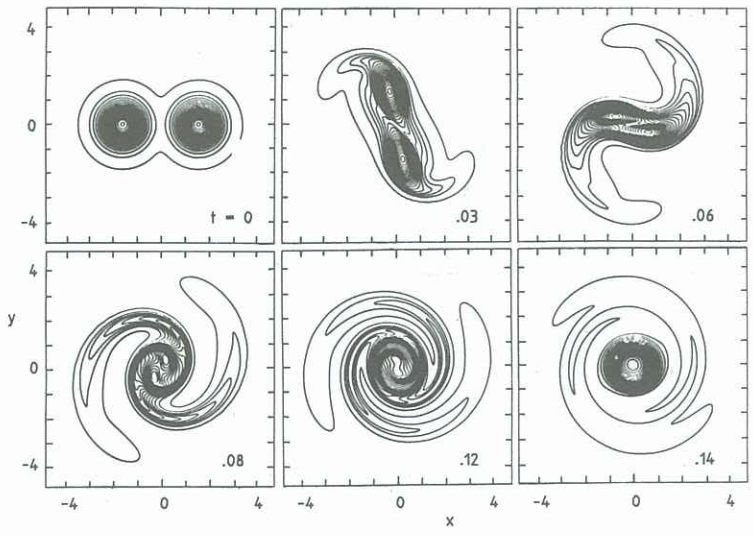

Figure 1. Vorticity contours for merging of two vortices (M = 2) in an axisymmetric strain field. Re = $\Gamma/2\pi\nu$ = 640. Times t as shown. Minimum contour $|\omega_{min}|$ = 30. Contour interval $|\Delta\omega|$ = 30. x = r cos(θ), y = r sin(θ).

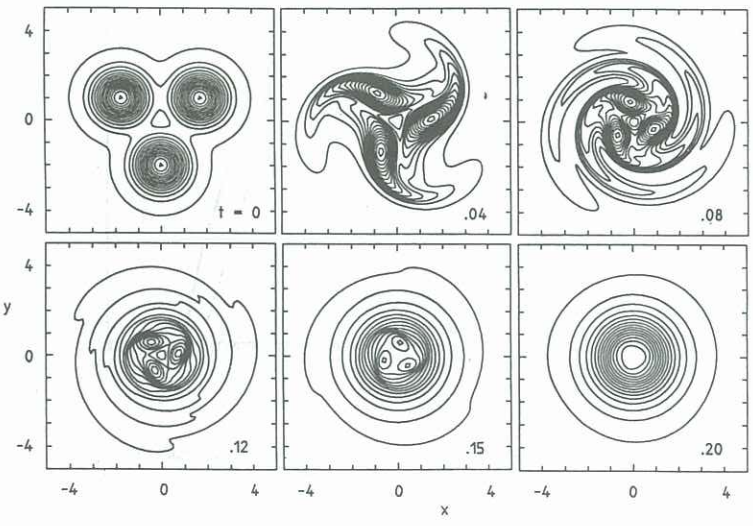

Figure 2. Vorticity contours for three-vortex (M = 3) merging in an axisymmetric strain field. For key see figure 2.

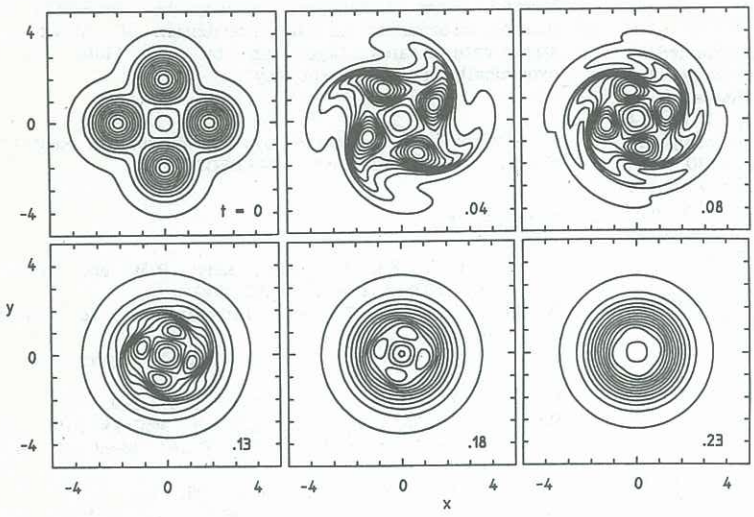

Figure 3. Vorticity contours for four-vortex (M = 4) merging in an axisymmetric strain field. For key see figure 2.

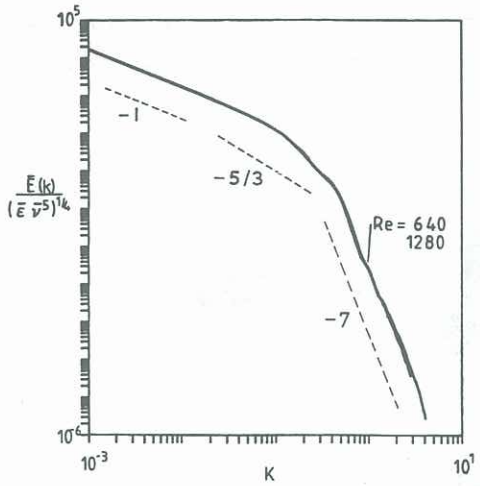

Figure 4. Energy spectra for two-vortex merging, M = 2, Re = 640, 1280

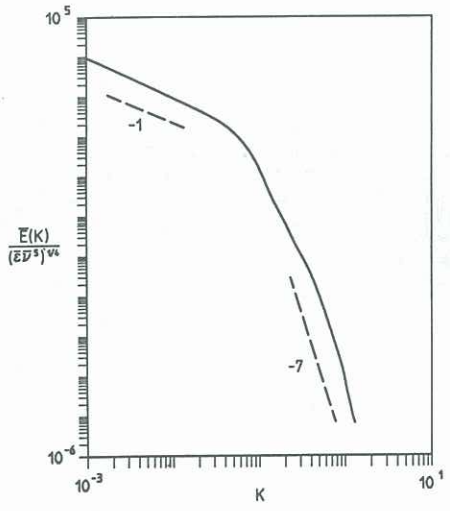

Figure 5. Energy spectrum for three-vortex merging, M = 3, Re = 640.

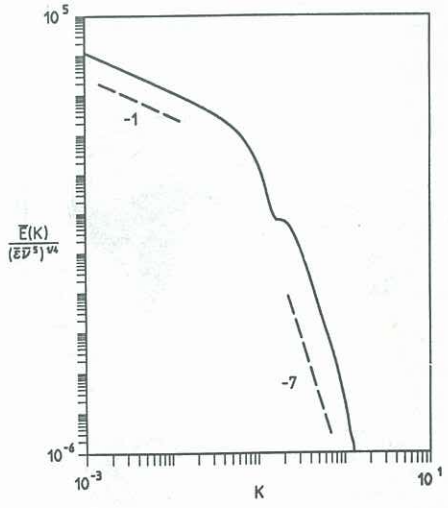

Figure 6. Energy spectrum for four-vortex merging, M = 4, Re = 640.